Dalton Transactions

Accepted Manuscript

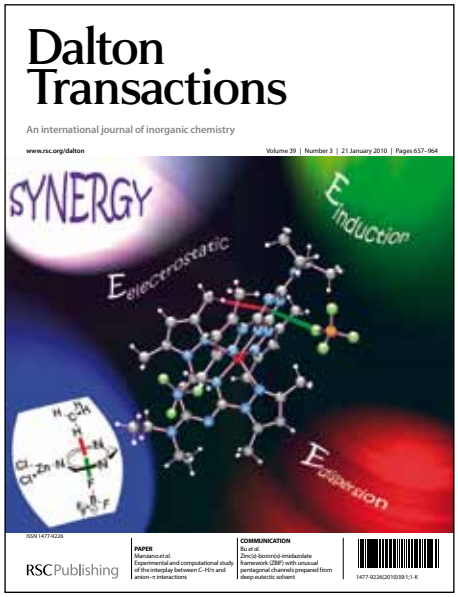

This is an *Accepted Manuscript*, which has been through the RSC Publishing peer review process and has been accepted for publication.

Accepted Manuscripts are published online shortly after acceptance, which is prior to technical editing, formatting and proof reading. This free service from RSC Publishing allows authors to make their results available to the community, in citable form, before publication of the edited article. This *Accepted Manuscript* will be replaced by the edited and formatted *Advance Article* as soon as this is available.

To cite this manuscript please use its permanent Digital Object Identifier (DOI®), which is identical for all formats of publication.

More information about *Accepted Manuscripts* can be found in the **Information for Authors**.

Please note that technical editing may introduce minor changes to the text and/or graphics contained in the manuscript submitted by the author(s) which may alter content, and that the standard **Terms & Conditions** and the **ethical guidelines** that apply to the journal are still applicable. In no event shall the RSC be held responsible for any errors or omissions in these *Accepted Manuscript* manuscripts or any consequences arising from the use of any information contained in them.

Journal Name

Dalton Transactions

Dynamic Article Links ►

Cite this: DOI: 10.1039/c0xx00000x

www.rsc.org/xxxxxx

ARTICLE TYPE

Highly Efficient and Stable DSSCs of Wet-chemically Synthesized MoS_2 Counter Electrode†

Supriya A. Patil,[a] Pranav Y. Kalode,[a] Rajaram S. Mane,[a, b] Dipak V.Shinde,[a] Ahn Doyoung,[a] Cho Keumnam,[a] M. M. Sung,[b] Swapnil B. Ambade,[c] Sung-Hwan Han[a,*]

Received (in XXX, XXX) Xth XXXXXXXXX 20XX, Accepted Xth XXXXXXXXX 20XX
DOI: 10.1039/b000000x

A competitive power conversion efficiency of 7.01% is achieved for TiO_2-based dye-sensitized solar cells (DSSCs) using chemically stable and mechanically robust molybdenum *di*-sulfide (MoS_2) counter electrode, synthesized using a simple, scalable and low-temperature wet-chemical process, owing to its good redox reaction stability.

In dye-sensitized solar cells (DSSCs), thermally evaporated or drop-casted platinum (Pt) counter electrode (CE) is commonly favored due to its excellent electrocatalytic activity. The ever escalating cost, scarcity and mandatory high temperature annealing requirements of Pt, however remain a hurdle in the context of commercialization. Thus, it is imperative to replace Pt by an alternative eco-friendly and cost-effective CE that would exhibit comparable chemical stability and catalytic activity.[1-3] Various alternatives including conducting polymers, carbon materials, transition metals, inorganic materials, nitrides, carbides and most recently electrochemically reduced graphene oxide etc.,[4,5] have been explored as counter-electrodes in DSSCs. On the other hand, environmentally benign, abundant, and non-expensive transition metal *di*-chalcogenides (MX_2, M= Mo, W and X = S, Se), sulfides and selenides are under extensive investigations due to their strong catalytic activities and potential applications including solar cells, light-emitting diodes, chemical sensors, thermoelectric devices, lithium-ion batteries, fuel cells and non-volatile memory devices, etc.[6,7] Among them, molybdenum disulfide (MoS_2), that typically is a two-dimensional, layered transition metal sulfide, exhibits hexagonal structure in which a sheet of Mo atoms is sandwiched between two hexagonally packed sulphur layers. The bonding between three stacked atomic layers (S-Mo-S) is covalent and held together by weak Vander Waals interactions. Moreover, with indirect band gap energy of 1.2 eV, it is a semiconductor with tremendous potential in the areas of photovoltaics and photocatalysis.[7-8] Most importantly, it can be synthesized at low temperatures using wet chemical methods.[8]

[a]*Inorganic Nanomaterials Laboratory, Department of Chemistry, Hanyang University, Seongdong-gu, 133791Seoul, Republic of Korea Email: shhan@hanyang.ac.kr,* [b]*Centre for Nano-materials & Energy Devices, School of Physical Sciences, SRTM University, 431606, Nanded, India Email: rsmane_2000@yahoo.com,*
[c]*Chonbuk National University, Jeonju, Korea.*

†Electronic Supplementary Information (ESI) available: Experimental procedures including structural characterizations and supplementary figures (Fig. S1-S5).

Despite the few reports of DSSCs of CE based on MoS_2–carbon composite (synthesized *in-situ* by hydrothermal method at 200℃ for 48 h) with power conversion efficiencies (PCE) of 7.59% and 7.69%, [9] surprisingly, literature on DSSCs with solution-processed pristine MoS_2 CE is still inadequate.[10] In this study, we introduce a simple, scalable (2.5 x 10 cm^2) and reproducible synthesis method for the fabrication of (pristine) MoS_2 CE using low-temperature, wet chemical route. This work is in continuation with our research focus on development of low-temperature chemical synthesis of DSSC components.[11] The performance of TiO_2-based DSSCs with MoS_2 CE exhibit an impressive 7.01% PCE that is comparable to DSSCs with Pt CE (7.31%), on account of excellent electrocatalytic activities (I_3^- reduction) of MoS_2.

MoS_2 CE was fabricated by immersing the pre-cleaned fluorine-tin-oxide (FTO) substrates in the reaction beaker containing appropriate concentrations of molybdenum (V) chloride and thioacetamide in ethanolic solution at 70℃ for 7 h (Fig. S1†). On completion of the reaction were taken off, washed with ethanol, distilled water and dried with argon gas prior to use. The Pt CE was freshly synthesized using a drop-cast method reported previously.[10] In brief, a thin TiO_2 blocking layer (100 nm) was deposited onto FTO by immersing the FTO in 0.1M $TiCl_4$ for 45 min at 70℃ and annealed at 450℃ for 30 min in air. A TiO_2 layer (4 μm) with average particle size of~20 nm was coated by the doctor blade method. Light scattering TiO_2 layer (thickness ≈ 3 μm) was applied over the previously deposited TiO_2 and sintered

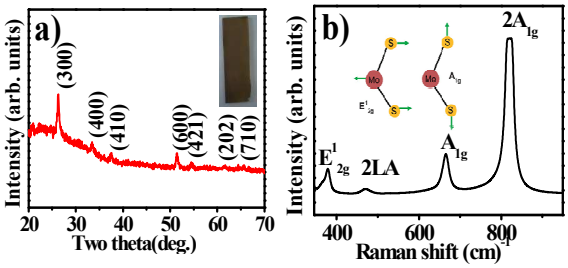

Fig.1 a) XRD pattern (inset: photoimage of MoS_2 CE), and b) Raman spectrum (inset: cartoon image of active modes) of MoS_2 CE.

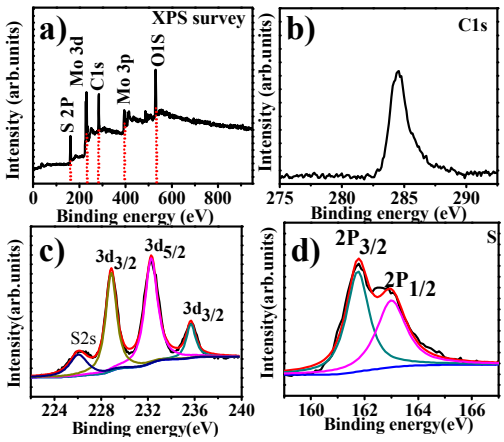

Fig.2. XPS plots of MoS_2 CE a) Survey, b) carbon, c) molybdenum and d) sulphur

.

again at 450℃ for 30 min. Prepared TiO_2 photoanode was dipped in 0.3 mM N719 (ethanol + acetonitrile) dye for 24 h to prepare a dye cell. The DSSCs were fabricated by injecting liquid electrolyte (0.05M I_2, 0.1 M LiI, 0.6M tetrabutylammonium iodide, and 0.5M 4-tert-Butylpyridine in acetonitrile) through an aperture between the dye–sensitized TiO_2 electrode and the CE (MoS_2 & Pt CEs, individually). The Field-emission scanning electron microscopy analysis revealed that the fabricated MoS_2 CE consists of densely packed nanocrystallites of 50-200 nm diameters. Fig. S2† (a~d) demonstrates that CE surface is free of cracks and nanocrystallites are stacked one above other with 100 nm thickness. This would propagate unperturbed charge transport. Grain size of 5-10 nm is evidenced from high-resolution transmission electron microscopy images (Fig. S2e-f†). X-ray diffraction (XRD) pattern of MoS_2 CE (Fig. 1a) obtained on glass substrate shows hexagonal crystal structure with a molybdnite mineral-type form (JCPDS No=731508). The diffraction at 2θ = 26.2° (300) is of higher intensity compared to others (33.4°, 37.5°, 51.35°, 54.4° and 61.5°, 65.5° and 78.4°) reflecting strong orientation along *a*-direction. MoS_2 phase is also confirmed from the selected area electron diffraction (SAED) pattern and the lattice spacing of 0.35 nm, obtained from the SAED pattern (Fig. S2g†), agrees to *d*-spacing of (3 0 0) MoS_2 plane (JCPDS No-731508). Chemical 1:2 stoichiometry for Mo and S, approved from the energy-dispersive X-ray spectroscopy (Fig. S2h†) analysis, is again confirming the formation of MoS_2. A set of fuzzy rings due to random orientation of the crystallites corresponding to diffraction from different planes is corroborating its nanocrystalline nature. Raman characteristic peaks (Fig. 1b) at 376 cm^{-1}, 459 cm^{-1}, 654 cm^{-1} and 821 cm^{-1} correspond to E^1_{2g}, 2LA, A_{1g} and $2A_{1g}$ Raman modes of MoS_2.[15] The surface area obtained using N_2 adsorption–desorption isotherms (H1 type) of MoS_2 (scratched from the electrode) is 159.67 $m^2\ g^{-1}$ (Fig. S3†). A broad and diffused peak at 10-150 nm and sharp peak at ~0.36 nm (inset) in the pore-size distribution curve confirms nanoporous structure of MoS_2, which should naturally result into enhanced redox reactions. Hall measurement (Fig. S4†) carried out at 300K revealed *p*-type conductivity of MoS_2 CE (conductivity= 2.6 x 10^{-4} Ω.cm^{-1}, charge mobility= 2.1 cm^2/Vs, Hall coefficient= 8.05 x 10^3 m^2/C and surface charge concentration= 2.32 x 10^{10} cm^2). The XPS spectrum of the MoS_2 CE is presented in Fig. 2a. In the C1s spectra (Fig. 2b) peaks at 285.1 eV to 286.1 eV binding energies are due to C-C, C-H and C-O bonds, respectively. The Mo3d signal (Fig. 2c) consists of two doublets. Doublet (Mo3d5/2= 229.4 eV; Mo3d3/2 = 232.6 eV) at a relatively low binding energy can be assigned to the Mo ion in the +4 oxidation state whereas the other doublet (Mo3d5/2= 232.6 eV; Mo3d3/2= 235.8 eV) is attributed to the Mo ion in MoO_3 which could possibly be formed in due course of redox reactions. Furthermore, peaks at binding energies 162.2 and 163.3 eV are assigned to the spin–orbit couple $S2p_{3/2}$ and $S2p_{1/2}$, respectively (Fig. 2d). These XPS signals are consistent to values reported elsewhere,[11] corroborating the formation of defect-free MoS_2.

The electrocatalytic activity and stability of MoS_2 CE for iodide reduction in relation with Pt CE are investigated using cyclic voltammetry (CV) and other electrochemical measurements using symmetrical sandwich-type configuration. The CV spectra (Fig. 3a) for the Pt and MoS_2 CEs in I_3^-/I^- redox electrolyte at 10 mVs^{-1} scan rate shows distinct cathodic peak potential of MoS_2 and Pt CEs at -0.125 and -0.127 V, respectively, supporting that the electrocatlytic activity of MoS_2 is comparable which is attributed to its relatively higher surface roughness compared to much smoother Pt (discussed later). Here, the anodic peak is responsible for $3I^-$ formation whereas cathodic peak produces $2I_3^-$ after accepting two electrons.[12] On the other hand, closely matched peak current densities of MoS_2 (-6.35 mA/cm^2) and Pt (-6.41 mA/cm^2) confirms the competitive electrocatlytic activity, as well as similar chemical capability of MoS_2 (in comparison to Pt) to reduce *tri*-iodide to iodide. Moreover, with increase in scan rate from 10 to 250 mVs^{-1} (Fig. 3b), the overall enclosed area of voltammogram for MoS_2 CE increases along with current density, indicating that at high scan rate, inner sites of MoS_2 also become reactive.[13] The higher peak current densities and lower peak-to-peak (E_{pp}) separation value (Table 1) confirm that MoS_2 offers remarkable electrocatalytic activity for the reduction of I_3^-. Furthermore, the unaltered curve shape and almost constant

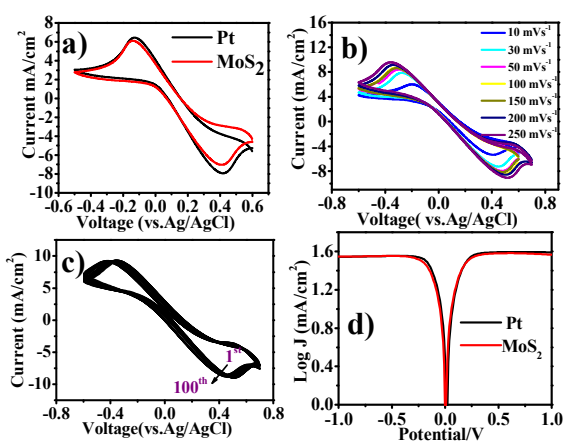

Fig. 3. CVs a) for I_3^-/I^- redox system using Pt, MoS_2 CEs, b) at

varying scan rates, c) durability test for 100 consecutive cycles at 10 mVs^{-1} scan rate, and d) Tafel polarization curves of symmetrical cells obtained with Pt and MoS_2 CEs.

current density for 100 cycles carried out at sweeping rate of 10 mVs^{-1} (Fig. 3c) confirms excellent electrochemical stability of the MoS_2 CE in the I^-/I_3^--based electrolyte system. In the Tafel polarization curves (Fig. 3d), a larger slope in the anodic and cathodic stream indicates nearly the same exchange current (J_o).[12] Apparently, the calculated J_o also follows the order of MoS_2>Pt, which is consistent with short-circuit current density (J_{sc}) value, suggesting that the MoS_2 CE has similar electrocatlytic activity to Pt CE. To further elucidate the catalytic activities of CEs on the reduction of *tri*-iodide, EIS experiments were carried out using symmetric cells fabricated with two identical electrodes (CE/electrolyte/CE). The Nyquist plots (Fig. 4a) for symmetric cells with MoS_2 CE illustrate impedance characteristics, in which two semicircles are observed in the higher (left) and lower (right) frequency regions. According to the Randles-type circuit (see S5†), the low-frequency intercept on the real axis represents the series resistance (R_s). The left arc arises from the R_{ct} at the CE/electrolyte interface, which changes inversely with the catalytic activity of MoS_2 CE on the reduction of *tri*-iodide, and the corresponding constant phase element (CPE), while the right arc arises from the diffusion impedance (W1) of the I_3^-/I^- redox couple in the electrolyte. The impedance values presented in Table S1 of ESI† are calculated using total surface area of catalysts on the electrode of the dummy cell. The obtained R_s value for MoS_2 CE (23.51 Ω cm^2) is lower than Pt CE (26.73Ω cm^2), indicating good catalytic activity on the reduction of *tri*-iodide. The R_{ct} values of MoS_2 and Pt CEs are 18.50 and 22.88 Ω cm^2, respectively. Here, W1 is increased from MoS_2 CE (1.8 Ω cm^2) to Pt CE (2.3 Ω cm^2), suggesting that the diffusion coefficients of *tri*-iodide is varying in the inverse order. Overall, the catalytic activity obtained from EIS and CV data is consistent. This strongly suggests that MoS_2 CE would be a good alternative to replace expensive Pt CE in DSSCs.

Fig. 4c presents the current density-voltage (*J–V*) curves of DSSCs based on MoS_2 and Pt CEs under illumination at 100 mW cm^{-2}. The obtained PCE parameters are summarized in Table 1. DSSCs employing MoS_2 as CE, exhibited excellent PCE of 7.01% owing to J_{sc} of 18.46 mA/cm^2, open-circuit voltage (V_{oc}) of 0.68 V, and fill factor (*ff*) of 0.58. This performance is close to that obtained for DSSCs having Pt CE (PCE= 7.31 %). Slight variations in V_{oc} followed by J_{sc} values for DSSCs of both CEs are attributed to; a) higher surface roughness of MOS_2 (19±0.25 nm) compared to Pt (6 nm) (Fig. S6†), b) nanoporous nature of MoS_2 CE in contrast to planar Pt CE, and c) *p*-type conductivity of MoS_2. The incident photon-to-current conversion efficiency curves of DSSCs based on Pt and MoS_2 CEs (Fig. 4b), exhibit similar nature as well as response, suggesting that almost similar catalytic activity is offered by MoS_2 CE.

CE	V_{oc} (V)	J_{sc} (mA /cm^2)	*Ff*	*η*(%)	E_{PP}/mV
Pt	**0.71**	**16.80**	**0.60**	**7.31**	**0.544**
MoS_2	**0.68**	**18.46**	**0 .58**	**7.01**	**0.539**

Table1. The extracted performance parameters for the TiO_2-based DSSCs with MoS_2 and Pt CEs.

A summary of results obtained in this work and other reported literature involving MoS_2-based CEs (composites) is compiled in Table S2†. It is noteworthy to mention that pristine MoS_2 CE, synthesized using wet chemical method at ambient temperature (70℃), has demonstrated remarkable TiO_2-based DSSCs performance and it is the first study of its kind, so far.

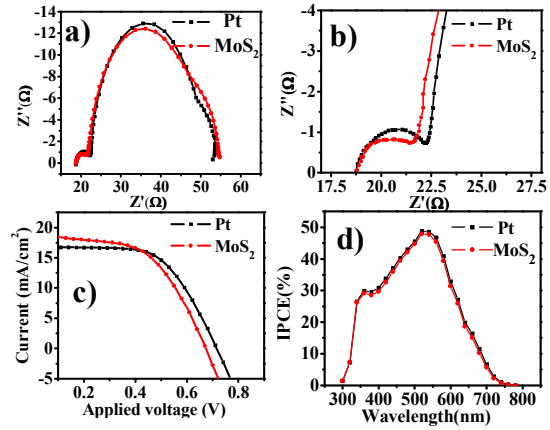

Fig. 4. a) Low, and b) high frequency range Nyquist plots, c) *J-V* and d) IPCE measurements of MoS_2 and Pt CEs.

In summary, we present for the first time, the use of wet chemically synthesized pristine MoS_2 CE in DSSCs. DSSCs based on mechanically robust MoS_2 CE with molybdnite mineral-type structure exhibited competitive power conversion efficiency of 7.01%, which is quite comparable to DSSCs of Pt CE (PCE= 7.31%). The MoS_2 CE presented in this work is quite promising and is a prospective candidate to replace highly expensive Pt as CE, owing to its comparable catalytic properties and most importantly, ease of fabrication at extremely low temperature.

This research was supported by Basic Science Research Program through the National Research Foundation of Korea (NRF) funded by the Ministry of Education (2013009768).

Notes and references

1. M. Gratzel, *Nature*, 2001, **414**, 338.
2. H. C. Sun, D. Qin, S. Q. Huang, X. Z. Guo, D. M. Li, Y. H. Luoand Q. B. Meng, *Energy Environ. Sci,* 2011, **4**, 2630.
3. H. Sun, Y. Luo, Y. Zhang, D. Li, Z. Yu, K. Li and Q. B. Meng,*J. Phys. Chem. C,* 2010, **114**, 11673.
4. Q. H. Li, J. H. Wu, Q. W. Tang, Z. Lan, P. J. Li and J. M. Lin,*Electrochem. Comm*, 2008, **10**, 1299.
5. A. Hagfeldt, G. Boschloo, L. Sun, L. Kloo and H. Pettersson, *Chem. Rev.,* 2010, **110**, 6595.
6. M. Chhowalla, H. SukShin, G. Eda, L. Jong Li, K. Ping Loh, H. Zhang, *Nature Chem.*,2013,**5**, 263.
7. Y. Shi, W. Zhou, A. Y. Lu, W. Fang, Y. H. Lee, A. L. Hsu, S. M. Kim,K . K. Kim, H. Y. Yang, L. J. Li, J . C. Idrobo, J. Kong, *Nano Lett*, 2012, **12**, 2784.
8. D. Kong, H. Wang, J. J. Cha, M. Pasta, K. J. Koski, J. Yao, Y. Cui, *Nano Lett*, 2013, **13**, 1341.
9. A. Hagfeldt, G. Boschloo, L. Sun, L. Kloo and H. Pettersson, *Chem. Rev.,* 2010, **110**, 6595.
10. A. Kay, M. Gratzel, *Sol. Energy Mater. Sol. Cells,* 1996,**44**, 99.
11 (a) S. B. Ambade, R. B. Ambade, R. S. Mane, G.W. Lee, S.F. Shaikh, S. A. Patil, O.S. Joo, S.H. Han and S.H. Lee, *Chem. Comm.***,** *2013,***49***, 2921.*(b) K. S. Liang, R. R. Chianelli, F. Z. Chien and S. C. Moss, *J. NonCryst. Solids,*1986,**79**, 251.
12 F. Gong, H. Wang, X. Xu, G. Zhou, and Z.S. Wang, *J. Am. Chem. Soc*. 2012, 134, 10953.
13 (a) C. W. Kung, H.W. Chen, C.Y. Lin, K. C. Huang, R.Vittal,

and K.C. Ho, 2012,**6,** 7016**.**(b) G. Yue, J.Y. Lin, S.Y .Tai, Y. Xiao, J . Wu, *Electrochemical Acta,* 2012, **85**,162.

Graphical abstract